

Copyright 1999 Society of Photo Instrumentation Engineers.

This paper was published in SPIE Proceedings, Volume 3778 and is made available as an electronic reprint with permission of SPIE. One print or electronic copy may be made for personal use only. Systemic or multiple reproduction, distribution to multiple locations via electronic or other means, duplication of any material in this paper for a fee or for commercial purposes, or modification of the content of the paper are prohibited.

Structured Polymer/Liquid Crystal for Switchable Diffractive and Micro Optics

Darius Subacius, Jay E. Stockley and Steven A. Serati

Boulder Nonlinear Systems, Inc.
450 Courtney way, #107
Lafayette, CO 80026

ABSTRACT

Polymer dispersed liquid crystals are generally described as a system with an isotropic liquid crystal (LC) droplet distribution in a polymer matrix. Using masked ultraviolet light and/or applied electric field a structured polymer/LC phase separation can be achieved. One technological advantage is the potential for integrated polymer/LC devices. This approach can be used to manufacture miniature switchable optical components such as diffractive gratings and switchable microlenses.

We investigate switchable diffractive gratings based on a structured polymer/LC system. LC director modeling is used to take into account the polymer regions and electric field orientation when the device thickness is comparable with the electrode period. Optical diffraction properties are compared with results of the theoretical modeling.

Keywords: liquid crystal, diffractive optics, polymer/liquid crystal structure, fringing fields, director modeling

1. INTRODUCTION

Liquid crystal (LC) spatial light modulators are primary used in display applications. However, recently LC devices have gained increasing importance in numerous non-display applications such as diffractive optics¹⁻⁴, optical processing, optical switching, non-mechanical beam steering⁵, voltage controlled focusing, and adaptive optics. Liquid crystal SLMs have the advantages of low voltage and low power consumption, along with large refractive index modulation. Depending on the liquid crystal material used and on modulator geometry, electro-optic modulation of phase, state of polarization, and intensity can be achieved. LC diffractive gratings are electrically controlled and exhibit the potential for high diffraction efficiency. They are usually fabricated using a few approaches: surface relief structure filled with LC^{3,4}, patterned electrodes^{1,2} and patterned surface alignment⁶. Another approach is to write the holographic grating in polymer dispersed liquid crystal, see for example ⁷ and references there.

In polymer dispersed liquid crystal (PDLC) modulators LC droplets are dispersed isotropically in a polymer matrix⁸⁻¹⁰. Device operation is achieved by electrical control of LC refractive index in droplets and, as a consequence, light scattering. Many new applications for diffractive and micro-optics can be envisioned if structured polymer/LC phase separation is achieved. In that case LC and polymer areas would be arranged in a predetermined manner with switchable LC regions and passive polymer regions. This phase separation was applied to isolate pixels in liquid crystal displays¹¹⁻¹⁴ to achieve wider viewing angle, rugged display structure, etc.

In this paper we discuss a few types of integrated polymer/LC devices from a fabrication technology standpoint. Experimental results of an electric field induced structured LC/polymer phase separation are presented to create various integrated optical microstructures. To explain the optical properties, LC director modeling is used. For high resolution devices LC molecule orientation is defined not only by surface

alignment, but also by the anchoring on polymer walls. When the electrode spacing approaches the pixel size, the electric field distribution in the anisotropic LC medium becomes complicated and numerical techniques are required to model the electro-optic properties of the device^{15,16}.

2. STRUCTURED LC/POLYMER PHASE SEPARATION

In polymer dispersed LC systems, for a review see^{8,9}, the initial mixture consists of LC mixed with a UV curable monomer (sometimes photoinitiator is added). The proportion of the mixture can be varied to obtain different concentration, size, and other parameters of LC droplets in PDLC. The mixture is filled into the cell with ITO coated substrates and exposed to UV radiation. The UV exposure can be performed in the absence of an applied field, as well as in an applied field. After the UV irradiation, the monomer crosslinks forming a polymer, at the same time as the phase separation occurs. Liquid crystals can separate forming spherical droplets in a polymer matrix. The droplets will have different diameters (usually in a range of 1 to 10 micrometers) and are uniformly dispersed within the polymer.

PDLC is useful in electro-optical devices because it can be switched electrically from a light scattering “off-state” to a highly transparent “on-state”. The polymer matrix is optically isotropic and has a refractive index n_p . Liquid crystal in microdroplets is optically uniaxial and is characterized by ordinary and extraordinary refractive indices. Since the diameters of LC droplets are comparable to the wavelength of the light, the light is scattered in the off-state, when there is no matching of refractive index. Upon application of an electric field, the liquid crystal director in each droplet orients along the field, and the refractive index of the droplets becomes ordinary refractive index n_o . If $n_p \approx n_o$, the film will be transparent.

Some new applications in micro- and diffractive optical elements could be addressed if phase separation in PDLC could be arranged in some predetermined manner. This would create switchable optical elements inside of the solid polymer matrix, opposite to the isotropic dispersion of LC droplets in the polymer matrix in regular PDLC devices. Considering optical arrays, incident light would be diffracted in fixed directions, versus diffused scattering in regular PDLC.

The structured polymer/LC phase separation is an integrated one step process, compared to the other types of diffractive LC elements mentioned above. Initially the LC and monomer mixture is filled into the cell and after, the polymerization and separation process is applied.

The structured polymer/LC separation can be achieved using a few techniques schematically presented in Fig.1. One approach (Fig.1a) is to use a photomask¹¹⁻¹³. The cell filled with a mixture is illuminated with ultraviolet light (UV) through the photomask with a pattern. In the illuminated areas monomer crosslinking occurs creating polymer rich regions, and LC is expelled into dark regions.

Another approach (Fig.1b) to create varying light distribution in the sample is to use interfering coherent optical beams. In this case switchable volume holograms are created in PDLC⁷. In thick films and small period patterns, the Bragg diffraction regime can be achieved with diffraction efficiency 70-95%⁷. The second approach has the advantage of higher resolution and the possibility to create a slanted grating. In the first approach the resolution is limited not only by the photomask, but also by the diffraction effects of UV light. Before reaching a few micron thick LC/monomer layer, diffracted light propagates through a comparably thick glass substrate.

To create switchable micro- and diffractive optics elements we used a third approach developed by the researches at the Liquid Crystal Institute¹⁴. Schematically it is represented in Fig. 1c. Voltage is applied across the cell with patterned indium tin oxide (ITO) electrodes. An electric field distribution in the LC/monomer layer and subsequent blanket UV- irradiation result in formation of polymer walls in the interpixel regions of the SLM. In these mixtures phase separation usually occurs upon cooling from the isotropic state into the heterogeneous state. The phase separation reduces the concentration of LC in the interpixel region. A possible physical mechanism of LC and monomer separation is different dielectric constants of the materials¹⁴. In the electrode region the electrostatic energy density stored by the single

pixel capacitor can be approximated by $W = \frac{1}{2} \int_V \epsilon E^2 dv$, where ϵ is the dielectric constant of the

material, E is the electric field strength, and V is pixel volume. The energy is minimized by forcing the material with higher ϵ out of the pixel region. As a consequence, electric field strength and dielectric

properties of LC and monomer determine the grating formation. Another driving force for phase separation is the electro-conductive effect. Ions present in the mixture create convection, helping phase separation.

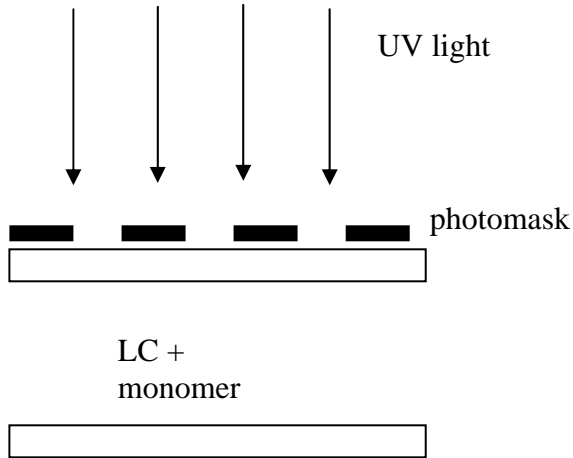


Figure 1a. Structure formation using photomask

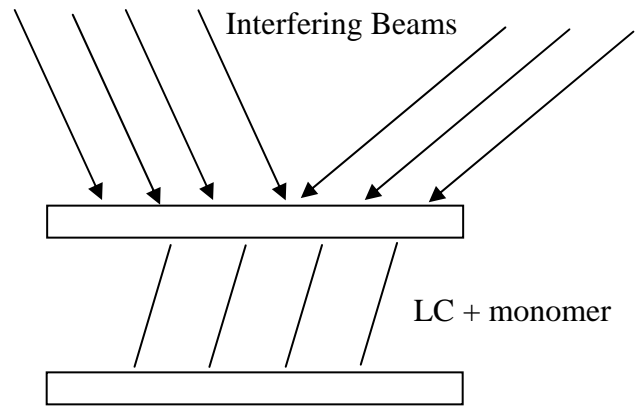


Figure 1b. Holographic grating in PDLC

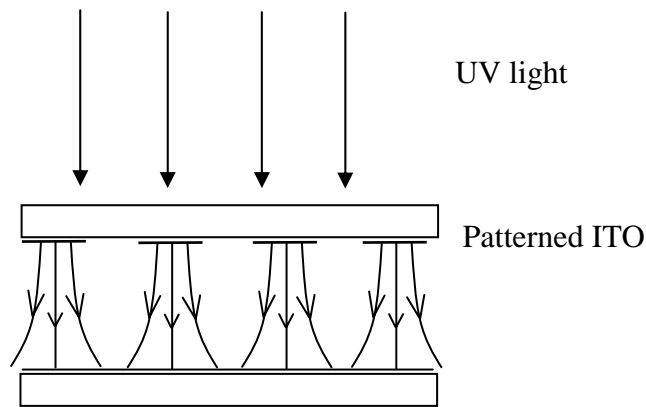


Figure 1c. Structure formation using electric field distribution

3. EXPERIMENTAL RESULTS

To fabricate swichable LC micro- or diffractive structures in a polymer matrix we used the technique¹⁴ shown on Fig. 1c. A mixture of monomer Norland Epoxy NOA65 (Norland Products, Inc.) and nematic liquid crystal E7 (EM Industries) was used. Norland Epoxy is an isotropic material. We also investigated reactive liquid crystal RM60 (EM Industries.), which exhibits a nematic phase over a temperature range. Using this material, an optically birefringent polymer matrix is fabricated. Using polymerized LC different diffractive structures can be obtained, for example, grating polarizing beam splitter¹⁷.

The mixing ratio was adjusted to the electrode fill ratio, depending on the pattern. Below we report results for E7/NOA65 mixtures. For a one dimensional array with $12\mu\text{m}$ electrode and $12\mu\text{m}$ spacing the mixture 60/40 % of E7/NOA65 was used. For a hexagonal grid of circles an 80/20 % mixture was used. The refractive indices of E7 for extraordinary and ordinary beams are 1.746 and 1.522, respectively ($T = 20^{\circ}\text{C}$, $\lambda = 589\text{nm}$) and $n = 1.524$ for NOA65. The mixture is filled into a cell with an ITO electrode pattern. The substrates are coated with polyimide and buffed to provide LC alignment. The thickness of the cells was set at $d = 4\mu\text{m}$ for the linear array and $d = 2.5\mu\text{m}$ for the hexagonal structure. The mixture is filled at elevated temperatures (90°C) and cooled down slowly in an applied electric field and observed under a polarization microscope. The phase separation temperature depends on the LC/polymer concentration¹⁴. Because the LC is optically birefringent and the monomer is isotropic, field induced monomer and liquid crystal separation can be visualized under the microscope: LC regions are located in electrode areas and the monomer is pushed out into the interpixel regions. Upon cooling to room temperature the cells were exposed to UV light to fix the structure.

Figures 2a and 2b show the obtained LC/polymer grating with LC separated in the electrode region and polymer in the interpixel region. Polymer walls are optically isotropic and do not transmit light between crossed polarizers. LC regions are birefringent and become bright when the device is rotated between crossed polarizers, Fig 2b. The buffing direction is parallel to the electrodes, and LC molecules are aligned in this direction. In Figure 2a the bright areas near polymer walls correspond to the complicated 3-D director orientation in that region. These distortions could be explained by the anchoring of LC molecules on polymer walls. In such a polymer/LC structure LC regions are confined not only by the cell substrates but also by the polymer walls in the interpixel region.

The liquid crystal regions are wider than electrode area because the LC concentration in a mixture was larger than that of polymer.

For comparison, in Figure 2b an area with the unaddressed electrode is presented where the LC droplets are dispersed isotropically in a polymer matrix as in regular polymer dispersed LC devices.

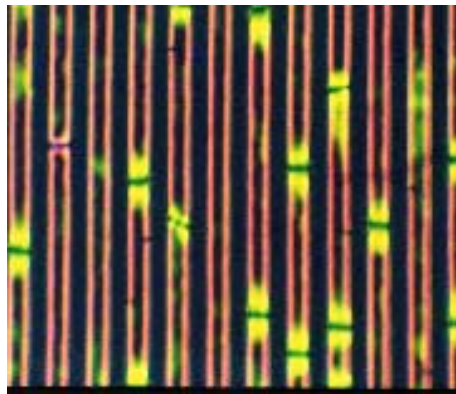


Fig.2a.

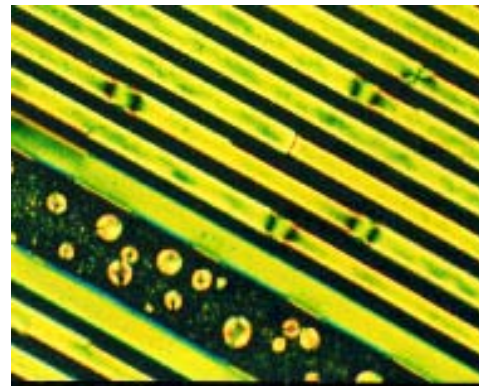


Fig.2b.

Fig.2 Microscopic photographs of the liquid crystal regions separated by the isotropic polymer walls between crossed polarizers. Fig.2a. walls are parallel to the analyzer, Fig.2b. walls are rotated for some angle from analyzer direction. Width of the electrodes is $12\mu\text{m}$ and spacing between is $12\mu\text{m}$, cell thickness is $4\mu\text{m}$.

For optical diffraction measurements we used a He-Ne laser ($\lambda = 633\text{nm}$), and light was incident normal to the cell. The incident light polarization was controlled by a polarizer, an analyzer was used to check the

diffracted light polarization. A photodiode was set at the location of diffraction maxima to measure intensity. The cell was driven by a signal generator, with the frequency usually set at 1kHz. The polymer/LC structure in the cell represents a phase grating. By changing applied voltage, the refractive index of LC regions is modulated, and the phase profile is changed. At high voltages, LC molecules are oriented homeotropic, with light sensing ordinary refractive index n_0 which is approximately equal to the polymer refractive index. Diffraction almost disappears.

Diffraction polarization properties confirm the assumption of complicated 3-D director orientation near polymer surfaces: diffracted light contains a small polarization component perpendicular to the incident light polarization.

The polymer/LC microstructure obtained using field induced phase separation in PDLC for a hexagonal pattern is presented in Figure 3. Circles correspond to holes in ITO patterning. After the separation, polymer regions are located in these spots, and are surrounded by LC areas. LC is oriented along the rubbing direction. The diameter of the dot is around $5\mu\text{m}$.

Under applied voltage the LC switches and the refractive index is modulated, at the same time, the polymer dots are fixed and their refractive index does not change.

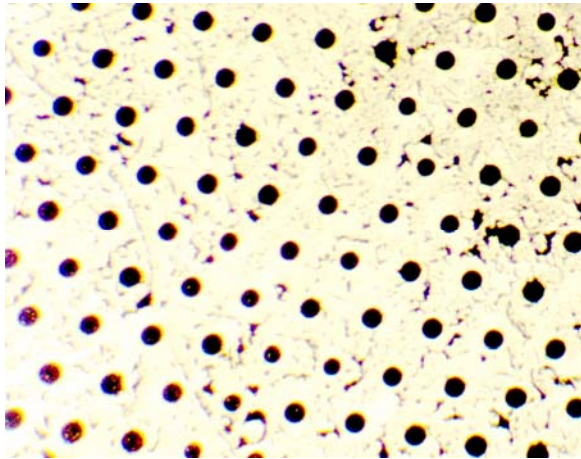


Fig.3a

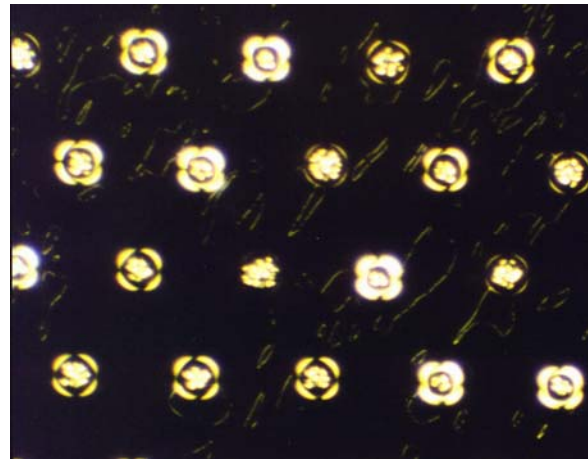


Fig.3b

Fig.3 Microscopic photographs between crossed polarizers of the structured polymer/LC separation with hexagonal pattern. Fig.2a. No voltage applied, LC alignment direction makes $\sim 45^\circ$ with polarizer, Fig.2b. Applied voltage $U=15\text{V}$, magnification in this photograph is 2X than former. Diameter of the dot is $5\mu\text{m}$.

Fig.3a shows phase separation with a hexagonal polymer dot pattern. The cell is rotated $\sim 45^\circ$ from the polarizer direction, the LC region is bright, the polymer dots are dark. Some polymer network is visible between grid points.

Fig. 3b is another sample of the same ITO patterning, where the structured phase separation is incomplete. For an applied voltage $U=15\text{V}$, liquid crystal regions are switched on, and between crossed polarizers they are dark the a picture. Inside of the polymer dots there are LC droplets, which show bright scattering.

The polymer/LC structures under consideration are fabricated using a structured electric field distribution in a cell. For higher resolution devices, depending on cell thickness, the fringing electrostatic fields should be taken into account. Field potential lines penetrate into the interpixel region, instead of the E-field being localized in the pixel region.

To illustrate fringing field and director distribution, we performed LC director simulations. Also we attempted to include LC anchoring effects on idealized polymer walls between electrodes.

4. FRINGING FIELDS AND DIRECTOR PROFILE MODELING

We used numerical simulations to take into account the fringing fields and LC director distortions in the inter-pixel region for 2-D model considering only the case when director deformations are confined in the xz plane. We have used a self-consistent model for the effects of an inhomogeneous electric field on the nematic liquid crystal grating.

For high resolution LC modulators the simplifying approximation that the medium is a homogeneous dielectric is not valid anymore. To obtain information about the extent of fringing fields, a quantitative analysis needs to consider the anisotropy of the liquid crystal.

The self-consistent model described here uses a finite difference approach^{15,16}. The medium is divided into a grid of points. For an anisotropic medium, the field is reduced due to dipole interactions. Laplace's equation becomes

$$\text{div}(\tilde{\epsilon} \text{grad } \Phi) = 0 \quad (1)$$

where Φ is the electrostatic potential and $\tilde{\epsilon}$ is the dielectric tensor.

First, an initial director distribution is assumed, which determines the dielectric tensor that is used in Laplace's equation. Taylor series expansion of Equation (1) about the grid points results in a finite difference equation which can be used to arrive at an iterative solution for the electrostatic potential.

$$\Phi(i, j) = \frac{1}{2(\epsilon_p + \epsilon_s)} \left[\epsilon_p \Phi(i, j+d) + \epsilon_s \Phi(i+d, j) + \epsilon_p \Phi(i, j-d) + \epsilon_s \Phi(i-d, j) \right] \quad (2)$$

Here, the indices i and j are the grid indices in the z and x (propagation direction and transverse direction) respectively. The subscripts p and s stand for parallel and perpendicular, respectively, and d is the distance between grid points (here assumed to be the same in both the x and z directions).

The electromagnetic field lines are determined from the gradient of the electrostatic potential.

$$\vec{E} = -\nabla \Phi \quad (3)$$

Once the field is known, the director distribution for the nematic liquid crystals is determined using a system of relaxation equations of elliptic form:

$$\gamma \frac{\partial}{\partial t} [n_a n_b] = K \nabla^2 [n_a n_b] + \frac{\Delta \epsilon}{4\pi} E_a E_b \quad (4)$$

Here n_a and n_b are the director components in the x or z direction. The subscripts a and b can both be x , z , or one of each. The viscosity coefficient is γ and K is the Frank-Oseen elastic constant. The electric field components are E_a and E_b . Finally, $\Delta \epsilon$ is the dielectric anisotropy. The equations are subject to the constraint that $n_x n_x + n_z n_z = 1$. The director distribution (obtained from the system of equations typified by Equation 4 above) is used to calculate a revised dielectric permittivity that is used in a new iteration of Laplace's equation¹⁶.

The basic algorithm is to begin with the dielectric tensor due to the director distribution at time $t=0$. Then, the initial estimate of the electrostatic potential is determined via convergence of the finite element formalism using Equation 2. The electric field is determined from the gradient of the electrostatic potential (Equation 3) and a director distribution is computed using the forward time, central difference method applied to the system of equations typified in Equation 4. The new director distribution is used to solve the inhomogeneous finite difference representation of Laplace's Equation¹⁶. From the electrostatic potential determined by convergence, the electrostatic field is recalculated using Equation 3 and substituted back into the system of equations used to determine the director distribution. This process is repeated until the potential function and the director distribution simultaneously converge.

In Figure 4 the LC director profile obtained by simulation for applied voltage $U = 5V$ is presented. In this figure and following modeling figures the electrode array consists of 4 μm lines and 2 μm spaces. The thickness of the liquid crystal medium is taken as 4 μm . Two electrodes are shown in the 12 μm region.

The first electrode is from $0.75\mu\text{m}$ to $4.75\mu\text{m}$ and the voltage is set to 0V . The second electrode is from $6.75\mu\text{m}$ to $10.75\mu\text{m}$ and the voltage is set to 5V . The top electrode is the ground electrode and voltage is always set to 0V . Boundaries to the left and right are assumed to wrap around (i.e. the pattern repeats itself in either direction). Initial LC alignment is planar along the x-axis with a small pretilt angle, the deformations are contained in the xz plane. Everywhere in simulations infinite anchoring energy is assumed. Solid lines represent the equipotential lines.

Figures 4 show that the electric field lines propagate into the interpixel region. The LC director field is slightly deformed from the initial orientation.

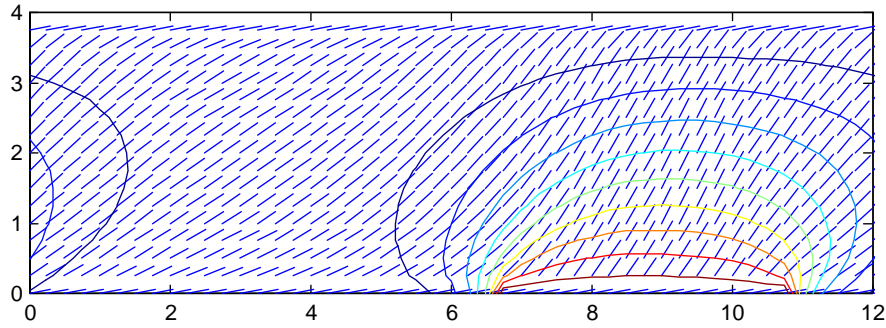


Fig. 4. Electrostatic potential lines and director profile for a 5V applied to the electrode array in binary addressing.

Fringing field penetration into the interpixel area depends on resolution and thickness of the device. When the thickness of the cell approaches the period of the structure, the electric field strength in the interpixel region becomes significant, hindering polymer and LC phase separation. Experimentally structured polymer/LC formation was attempted for higher resolution devices. However, as could be expected from simulation results, phase separation was not good. To fabricate structured polymer/LC separation we need the E-field to be localized in the pixel region.

Another interesting possibility is to use the fringing fields to shape polymer/LC structures across the cell thickness. Circular, conical, etc. structures could possibly be created. This could be of interest for fabrication of switchable microlens arrays, etc.

Anchoring effects.

For structured polymer/LC devices with higher resolution, LC director anchoring on polymer regions becomes important. The LC director is aligned not only by the cell substrates, but also by the polymer interface,

see Figure 2. Axially symmetric director alignment was used to improve the viewing characteristics of an LCD using a microcell structure¹¹. LC director alignment was set by the polymer walls of the microcell. In such a confined structure LC orientation is complicated to minimize elastic distortions. Anchoring effects influence LC electro-optical properties and switching characteristics.

Figure 5a illustrates the director orientation in the array with the polymer/LC structure at an applied voltage of $U = 5\text{V}$. On the left pixel a voltage $U = 0\text{V}$ is applied. Director alignment is set by polymer walls and surface alignment. The right pixel is switched on, with the director aligned along the field.

Figure 5b illustrates the phase transmission function of the binary LC grating shown in Fig.5a. To obtain the phase profile $\Phi(x)$ in the near field we used a Jones matrix technique. The far field diffraction pattern can be obtained by a Fourier transform.

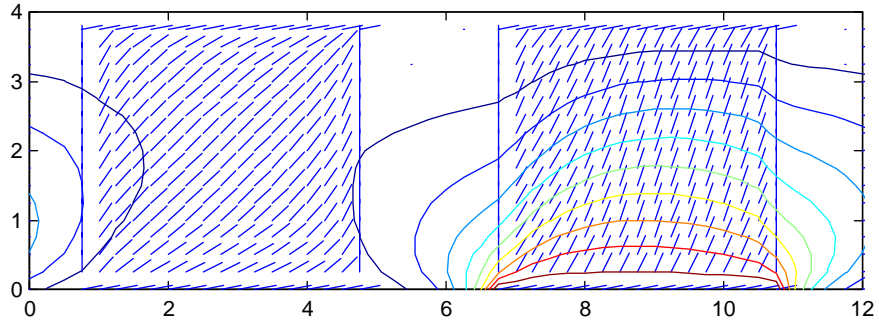


Fig. 5a LC director profile in the array with pixel separated structure in binary addressing, applied voltage $U = 5V$. Empty areas represent the isotropic walls.

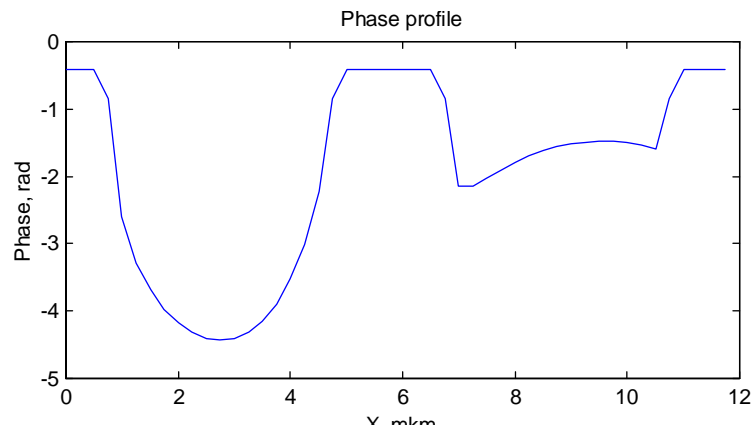


Fig. 5b Phase transmission profile in the near field corresponding to the director profile of Fig. 5a.

5. CONCLUSIONS

We have discussed the structured polymer/LC phase separation. A polymer/LC structure with switchable LC and fixed polymer regions can be fabricated using a patterned electric field in a cell. Contrary to conventional PDLC devices, the LC regions are arranged in a predetermined manner. This technique can be used to fabricate integrated, switchable LC micro- and diffractive optical components. Linear diffractive arrays and hexagonal microstructures were fabricated and optically tested. To understand the influence of the fringing fields for higher resolution devices and to take into account LC anchoring on polymer surfaces we have performed liquid crystal director modeling. Electric field distribution can be used to shape the polymer/LC regions in the cell.

The applications of this technology could be beneficial to switchable diffractive elements, beam steering and adaptive optics, microlenses, waveguides.

6. ACKNOWLEDGMENTS

This work is supported by Wright Laboratory, Wright-Patterson AFB contract number F33615-97-C-1140. Part of this research was also funded by Phillips Laboratory, Kirtland AFB, contract #F29601-98-C-0045.

7. REFERENCES

1. R.A. Kashnow and J.E. Bigelow, "Diffraction from a liquid crystal phase grating", *Appl. Opt.* **12**, pp.2302, 1973.
2. M.W. Fritsch, C. Kohler, G. Haas, H. Wohler, D.A. Mlynski, "Diffraction properties of rectangular phase gratings in a liquid crystal phase modulator", *Mol. Cryst. Liq. Cryst.* **198**, pp. 1-14, 1991.
3. E. Schulce, "Novel high-resolution spatial light modulators with limited spectral bandwidth for 2D and 3D image generation" *Proc. SPIE* **1988**, pp.44, 1993.
4. H. Murai, T. Gotoh, M. Suzuki, E. Hasegawa and K. Mizoguchi, "Electro-optic properties for liquid crystal phase gratings" *Proc. SPIE* **1665**, pp.230, 1992.
5. P.F. Mcmanamon, T.A. Dorschner, D.L. Corkum, L.J. Friedman, D.S. Hobbs, M. Holz, S. Liberman, N.Q. Nguyen, D.P. Resler, R.C. Sharp, E.A. Watson, "Optical phased array technology", *Proc. IEEE* **84**, pp. 268-298, 1996.
6. J. Chen, P.J. Bos, H. Vithana, and D.L. Johnson, "An electro-optically controlled liquid crystal diffraction grating", *Appl. Phys. Lett.* **67**, pp.2588-2590, 1995.
7. R.L. Sutherland, L.V. Natarajan, V.P. Tondiglia, R.T. Pogue, S.A. Siwecki, D.M. Brandelik, B.L. Epling, E. Berman, C. Wendel, and M.G. Schmitt "Holographic PDLCs for spatial light intensity modulation", *Proc. SPIE* **3633**, pp.226-233, 1999.
8. "Liquid crystals in complex geometries", ed. G.P. Crawford and S. Zumer (Taylor and Francis, London, 1996).
9. P.S. Drzaic, "Liquid crystal dispersions", (World Scientific, Singapore, 1995).
10. J. W. Doane, N. A. Vaz, B.-G. Wu and S. Zumer, *Appl. Phys. Lett.*, **48**, 269 (1986).
11. N. Yamada, S. Kohzaki, F. Funada, K. Awane "Axially symmetric aligned microcell (ASM) mode: electro-optical characteristics of new display mode with excellent wide viewing angle", *SID Digest of Technical Papers*, pp.575-578, 1995.
12. Y. Ji, J. Francl, W. J. Fritz, P. J. Bos, and J. L. West "Polymer walls in higher-polymer-content bistable cholesteric displays", *SID Digest of Technical Papers*, 611 (1996).
13. W.T. He, T. Nose and S. Sato, "Novel liquid crystal grating with a relief structure by a simple UV irradiation process", *Jpn. J. Appl. Phys.* **37**, pp.4066-4069, 1998.
14. Y. Kim, J. Francl, B. Taheri and J.L. West, "A method for the formation of polymer walls in liquid crystal/polymer mixtures", *Appl. Phys. Lett.* **72**, pp. 2253-2255, 1998.
15. G. R. Magyar, J. L. West, B. Taheri, Y. Kim and V. Bodnar, *SID Digest of Technical Papers*, 664 (1999).
16. A. Kilian and S. Hess, "Derivation and application of an algorithm for the numerical calculation of the local orientation of nematic liquid crystals", *Z. Naturforsch.* **44a**, pp. 693-703, 1989.
17. G. Haas, H. Wohler, M. W. Fritsch and D.A. Mlynski, "Simulation of two-dimensional nematic director structures in inhomogeneous electric fields", *Mol. Cryst. Liq. Cryst.* **198**, pp. 15-28, 1991.
18. H. Sato, H. Hotaka, T. Gunjima, Y. Tanabe, and M. Hirano, "Grating polarizing beam-splitter using polymerized liquid crystal", *Jpn. J. Appl. Phys.* **36**, pp.589-590, 1997.